Thymic output generates a new and diverse TCR repertoire after autologous stem cell transplantation in multiple sclerosis patients

Paolo A. Muraro,[1] Daniel C. Douek,[4] Amy Packer,[1] Katherine Chung,[1] Francisco J. Guenaga,[4] Riccardo Cassiani-Ingoni,[1] Catherine Campbell,[2] Sarfraz Memon,[5] James W. Nagle,[3] Frances T. Hakim,[5] Ronald E. Gress,[5] Henry F. McFarland,[1] Richard K. Burt,[6] and Roland Martin[1]

[1]Neuroimmunology Branch, [2]Information Technology Program, and [3]DNA Sequencing Core Facility, National Institute of Neurological Disorders and Stroke, [4]Human Immunology Section, Vaccine Research Center, National Institute of Allergy and Infectious Diseases, and [5]Experimental Transplantation and Immunology Branch, National Cancer Institute, National Institutes of Health, Bethesda, MD 20892
[6]Division of Immunotherapy, Department of Medicine, Feinberg School of Medicine, Northwestern University, Chicago, IL 60208

Clinical trials have indicated that autologous hematopoietic stem cell transplantation (HSCT) can persistently suppress inflammatory disease activity in a subset of patients with severe multiple sclerosis (MS), but the mechanism has remained unclear. To understand whether the beneficial effects on the course of disease are mediated by lympho–depletive effects alone or are sustained by a regeneration of the immune repertoire, we examined the long–term immune reconstitution in patients with MS who received HSCT. After numeric recovery of leukocytes, at 2-yr follow–up there was on average a doubling of the frequency of naive CD4+ T cells at the expense of memory T cells. Phenotypic and T cell receptor excision circle (TREC) analysis confirmed a recent thymic origin of the expanded naive T cell subset. Analysis of the T cell receptor repertoire showed the reconstitution of an overall broader clonal diversity and an extensive renewal of clonal specificities compared with pretherapy. These data are the first to demonstrate that long–term suppression of inflammatory activity in MS patients who received HSCT does not depend on persisting lymphopenia and is associated with profound qualitative immunological changes that demonstrate a de novo regeneration of the T cell compartment.

CORRESPONDENCE
Paolo Muraro:
murarop@ninds.nih.gov
OR
Roland Martin:
martinr@ninds.nih.gov

Abbreviations used: AUC, area under the curve; CNS, central nervous system; EDSS, expanded disability status scale; HSCT, hematopoietic stem cell transplantation; MRI, magnetic resonance imaging; MS, multiple sclerosis; RTE, recent thymic emigrant; TBI, total body irradiation; TREC, T cell receptor excision circle.

Multiple sclerosis (MS) is considered a T cell–mediated inflammatory demyelinating disorder of the central nervous system (CNS; reference 1), although other immune factors such as complement and antibodies as well as factors intrinsic to the CNS are thought to contribute to disease expression. MS mainly affects young adults and often leads to substantial disability at an early age, resulting in enormous socioeconomic costs. Most patients suffer from relapsing–remitting disease, which later evolves into a secondary chronic disease process. The role of autoimmune inflammation is probably more important during earlier stages of the disease, when CNS damage is still limited. Once the secondary progressive course has set in, in some aspects MS resembles a neurodegenerative disease with continuously increasing disability and more limited or no inflammation. Currently, there is no curative treatment of MS, particularly for patients with rapidly worsening disease. Immunomodulatory agents have been approved for relapsing–remitting MS but no treatment, even intense immunosuppression, appears to be effective during the later progressive disease stages. Phases I and II clinical trials have suggested that immune ablation followed by autologous hematopoietic stem cell transplantation (HSCT) can suppress brain inflammation in the majority of high-risk patients refractory to approved treatments and, in some, may also arrest or delay progression of clinical disability (2, 3).

The rationale for HSCT in autoimmune diseases has been the notion that intensive immune depletion could eliminate autoreactive

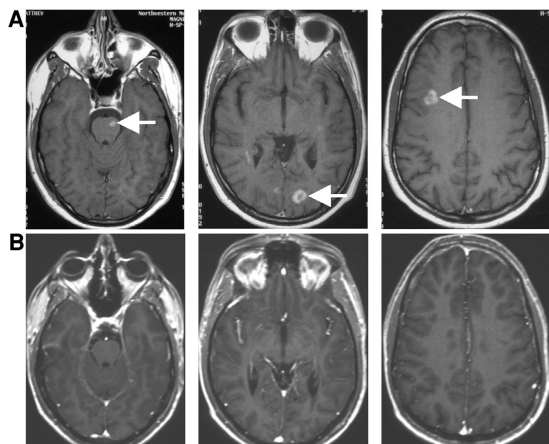The online version of this article contains supplemental material.

Figure 1. Resolution of inflammatory disease activity after HSCT. Representative contrast-enhanced MRI axial scans of the brain of patient 2 at pretransplant evaluation (top) and at 2-yr follow-up (bottom) illustrate a long-lasting resolution of inflammatory disease in this patient with high pretransplant activity (arrows point at 3 out of 17 total enhancing lesions present in the brain pretherapy; no enhancing lesions were detected after therapy).

immune cells irrespective of antigenic specificity and that regenerating the immune system from hematopoietic precursors could reestablish tolerance (4). However, available data on immune reconstitution in patients with autoimmune disease are limited to 1 yr of follow-up posttransplantation at most (5–8), and no study has demonstrated that HSCT can actually "reset the immunological clock" by detecting phenotypic or functional renewal of the immune repertoire during long-term clinical remission.

To address the question whether there is such immune regeneration in patients with MS who cease to present inflammatory disease activity after the treatment, we studied the mechanisms of long-term T cell reconstitution in seven patients with MS that we prospectively followed for up to 3 yr after receiving a high-intensity myelo- and immunoablative HSCT regimen (Table I and Fig. 1). Our results establish that HSCT goes far beyond mere immune ablation and provide evidence of extensive renewal of T cell repertoires after HSCT.

RESULTS

Leukocyte recovery

First, we assessed basic aspects of the patients' immune reconstitution by flow cytometry using leukocyte lineage and subpopulation markers. Because lymphocyte numbers are reconstituted early after HSCT (9), we expectedly found that mean absolute lymphocyte counts ($1.20 \pm 0.48 \times 10^3$ cells/μL blood) were already back to baseline levels at the 6-mo follow-up ($1.20 \pm 0.70 \times 10^3$ cells/μL) and remained stable at the 1-yr (mean $1.15 \pm 0.32 \times 10^3$ cells/μL) and 2-yr follow-ups ($1.34 \pm 0.49 \times 10^3$ cells/μL). At 6 mo and subsequent time-points, there were no significant changes from prether-

Table I. Demographic and clinical features of patients

Patient code	Gender/age	Disease course[a]	Clinical relapses in 2 yr before HSCT	Clinical relapses after HSCT	Clinical follow-up after HSCT
	yr		no.		mo
1	M/53	SP-MS	2	0	36
2	M/30	RR-MS	4	0	28
3	F/53	SP-MS	3	0	28
4	M/28	PR-MS	2	0	28
5	M/45	PR-MS	4	0	27
6	F/47	SP-MS	2	0	25
7	M/51	SP-MS	2	0	21

[a]PR-MS, progressive–relapsing MS; RR-MS, relapsing–remitting MS; SP-MS, secondary progressive MS.

apy in the proportions of CD3$^+$ T cells, CD19$^+$/CD20$^+$ B cells, NK (CD3$^-$CD56$^+$), NK T cells (CD3$^+$CD56$^+$), and CD14$^+$ monocytes (unpublished data). The CD4/CD8 ratios were significantly decreased at 6 mo after HSCT compared with baseline (mean 0.41 vs. 2.37; P < 0.001) due to reduced proportions of CD4$^+$ T cells in the early posttransplant phase. Consequent to the gradual normalization of CD4$^+$ and CD8$^+$ T cell absolute counts, CD4/CD8 ratios were reverting toward baseline levels at 1 yr (mean 0.73; P = 0.002) and were no longer significantly different at the 2-yr follow-up (mean 1.79; P = NS), in agreement with data on immune reconstitution in other diseases (10). The observed recovery of lymphocyte numbers indicated that the prolonged absence of new MS inflammatory disease activity after HSCT did not require a persistent lymphopenia.

Increased naive T cells and decreased central–memory T cells after posttransplant immune reconstitution

Whether protective or pathogenic, T cell effector functions are mediated by memory (peripherally primed) cells; therefore, elimination or reduction of memory cells is likely to reduce the number of pathogenic cells in a subject with an immune-mediated disorder. In contrast, the influx of de novo–generated naive cells is recognized as an important component of immune tolerance (11). To assess the effects of HSCT on the size of the naive and memory T cell pools, we used phenotypic markers that allow us to distinguish various functional differentiation stages, including naive (T$_{naive}$), central–memory (T$_{CM}$), and effector–memory (T$_{EM}$) cells (12). The longitudinal analysis of the frequency of these subpopulations after HSCT is shown in Fig. 2. At 6 mo posttransplant, there was a trend toward a reduction of naive (CD45RA$^+$/CD45RO$^-$/CD27$^+$) CD4$^+$ T cells (CD4 T$_{naive}$), consistent with the prevalence of effector–memory phenotypes resulting from homeostatic proliferation in a lymphopenic environment (13–15). Central–memory (CD45RA$^-$/CD45RO$^+$/CD27$^+$) CD4$^+$ cells (CD4 T$_{CM}$) decreased steadily during the posttransplant follow-up. The proportion of effector–
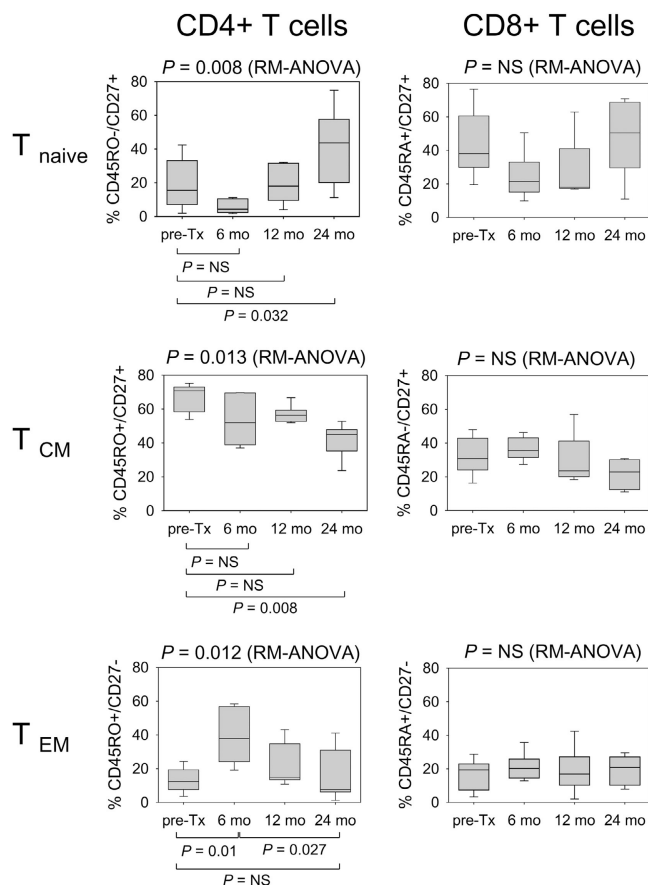
CD4+ T cells

CD8+ T cells

Figure 2. Phenotypic analysis of naive and memory T cell populations. All values are the percent expression of the indicated T cell subpopulation at pretherapy and follow-up time points. (left) Subsets of CD4$^+$ T cells and (right) subsets of CD8$^+$ T cells, each categorized as T_{naive}, naive T cells; T_{CM}, central–memory T cells; and T_{EM}, effector–memory T cells. The boundaries of the boxes indicate the 25th and 75th percentiles, the lines within the boxes indicate the median, and the whiskers mark the 10th and the 90th percentiles. We observed a statistically significant (greater than twofold) increase of CD4 T_{naive} and a decrease of CD4 T_{CM}.

memory (CD4$^+$/CD45RA$^-$/CD45RO$^+$/CD27$^-$) CD4$^+$ cells (CD4 T_{EM}) rose significantly at 6 mo after HSCT and later declined toward baseline levels after the gradual replenishment of the absolute CD4$^+$ T cell numbers. Of note, when we examined the net outcome at the end of the 2-yr follow-up, we found a more-than-doubled frequency of CD4 T_{naive} as compared with pretherapy (118% increase; P = 0.032). Correspondingly, CD4 T_{CM} cells were significantly decreased at 2 yr after therapy (by 38%; P = 0.008). The frequencies of CD4 or CD8 T_{EM} and of CD8 T_{naive} did not change significantly at the 2-yr follow-up compared with the baseline. The atypical effector–memory phenotype of oligoclonally expanded CD8$^+$ cells appearing posttransplant, as shown later, should be taken into account for the interpretation of these data. There was a trend to a decrease of CD8 T_{CM} percentages at the 2-yr follow-up (32% reduction), but the study was underpowered to assess the statistical signifi-

cance. Together, our analysis showed that approximately one fourth of the CD4$^+$ cell pool occupied by CD4 T_{CM} was repopulated by CD4 T_{naive} cells, leading to a 76% reduction of CD4 T_{CM}/CD4 T_{naive} ratios (from 4.72 to 1.12; P = 0.035). These data support the notion that HSCT can induce a phenotypic rejuvenation of the CD4$^+$ T cell repertoire.

Increased output of recent thymic emigrants (RTEs)

To determine the source of the increase of phenotypically naive CD4$^+$ cells, we took two approaches to assess the thymic versus peripheral origin of the reconstituted T cell pool. To identify RTEs in the CD4$^+$ subset, we first used as marker the expression of CD31 in combination with CD45RA and CD45RO, as described recently (16). The mean frequency of CD4 RTEs (CD4$^+$/CD45RA$^+$/CD45RO$^-$/CD31$^+$), reduced at 6 mo posttransplant, subsequently recovered and doubled from 18% at baseline to 36% at 2 yr after HSCT (P = 0.028; Fig. 3 A). To confirm and extend the analysis, we used a highly specific assay to measure the presence of de novo–generated T cells in peripheral blood based on the quantification of T cell receptor excision circles (TRECs). TRECs are stable DNA episomes formed during rearrangement of the TCRAD locus during T cell
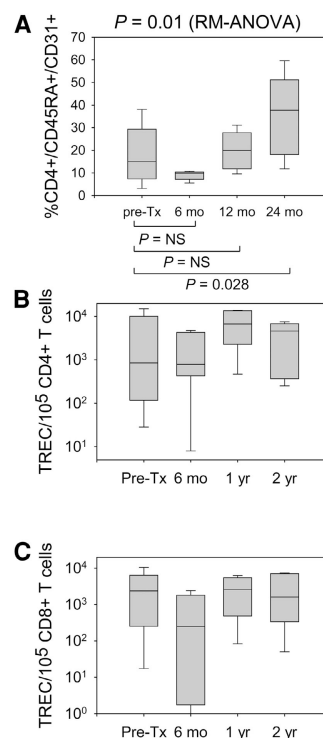

Figure 3. Measures of thymic output after HSCT. (A) Phenotypic identification of RTEs in the CD4$^+$ subset showed a significant increase of CD4$^+$ RTEs at 2-yr follow-up. (B) TCR excision circle (TREC) analysis showed full reconstitution and increases of CD4 RTE output at 2-yr follow-up. (C) Due to extensive peripheral cell division, CD8 TREC levels only recovered up to near-pretherapy levels. Age–related interindividual variance and the small number of patients precluded a statistical evaluation of TREC data.

differentiation in the thymus. Because TRECs do not replicate with cell division, they have been successfully used as a marker for RTEs (17). We followed the evolution of TREC levels after HSCT in purified CD4$^+$ and CD8$^+$ T cells (Fig. 3 B). As expected, TREC content was generally decreased in both subsets early (6 mo) posttransplantation, when immune reconstitution predominantly relies on peripheral expansion of the autologous graft. However, starting 1 yr after HSCT, CD4 TREC levels rebounded from a median of 848 TRECs/10^5 CD4$^+$ cells at baseline to 6,689 TRECs/10^5 CD4$^+$ cells at 1 yr and 4,602 TRECs/10^5 CD4$^+$ cells at the 2-yr follow-up (a 7.9-fold and 5.4-fold increase, respectively). Due to the small number of patients and interindividual variance (largely age-related), our study was underpowered to assess the statistical significance of this increase. Most patients recovered pretransplant CD8 TREC at the 1-yr follow-up and after, but there was no overall increase at the end of the 2-yr observation period (Fig. 3 C). When we examined the correlation of the frequency of phenotypically identified CD4$^+$ naive cells and CD4 RTEs, we found no correlation in the early (6 mo) posttherapy phase, but a strong correlation was reestablished at 1 yr (Pearson's $r = 0.982$ with P = 0.002) and further increased its significance at the 2-yr follow-up; $r = 0.988$ with P < 0.001). This observation established further evidence to suggest a true thymic origin for the observed phenotypic rejuvenation of the CD4$^+$ T cell repertoire.

Recovery of T cell receptor repertoire diversity

First, we followed the reconstitution of the peripheral blood TCR Vβ repertoire using a panel of TCR Vβ–specific monoclonal antibodies and flow cytometry at baseline and at the 6-mo, 1-yr, and 2-yr follow-ups. One patient showed a transient TCR Vβ expansion in the CD4$^+$ T cell subset (patient no. 1, Vβ17 at 6 mo after HSCT). In the remaining patients (e.g., patient no. 4; Fig. S1, available at http://www.jem.org/cgi/content/full/jem.20041679/DC1), the TCR Vβ profiles of CD4$^+$ T cells remained stable throughout the follow-up. In contrast, we frequently detected expansions of individual TCR Vβs after HSCT in the CD8$^+$ subset (Table II). These expansions were not associated with clinical or laboratory signs of infection or with MS relapses. After a 2-yr follow-up, reconstituted TCR Vβ repertoires of CD4$^+$ T cells were very similar to the pretransplant repertoires, showing in each patient <4% absolute difference of expression for each TCR Vβ. Due to the persistent expansion of CD8$^+$ T cells expressing individual Vβs, we detected larger differences in the 2-yr posttherapy profiles of TCR Vβ expression for the CD8$^+$ subset. Multidimensional scaling analysis illustrated how closely the reconstituted TCR Vβ repertoires resembled each individual's pretreatment profile for CD4$^+$ cells (Fig. S2, available at http://www.jem.org/cgi/content/full/jem.20041679/DC1). This trend was seen to be more limited when looking at CD8$^+$ cells.

To investigate in greater depth the evolution of the peripheral TCR repertoire after HSCT, we used TCRB CDR3

Table II. Significantly expanded TCR Vβ–expressing cells after HSCT

Patient	T subset	TCR	Pre–Tx[a]	6 mo after Tx	1 yr after Tx	2 yr after Tx
1	CD4$^+$	BV1	2.5	8.8[b]	ND	3.5
	CD4$^+$	BV17	10.5	**32.0**	ND	9.3
2	CD8$^+$	BV18	0.5	**6.1**	**2.2**	**2.0**
	CD8$^+$	BV20	2.6	**7.6**	**8.1**	**9.4**
4	CD8$^+$	BV1	5.7	4.2	**15.6**	9.8
5	CD8$^+$	BV8	6.9	**17.9**	**14.0**	**18.9**
	CD8$^+$	BV21.3	1.4	**3.6**	**2.9**	**6.6**
6	CD8$^+$	BV1	5.2	ND	**17.5**	9.9
	CD8$^+$	BV5.1	3.5	ND	**8.6**	**9.4**
7	CD8$^+$	BV5.1	1.75	**6.8**	4.7	ND
	CD8$^+$	BV23	0.3	**49.9**	**53.9**	ND

[a]Tx, treatment.
[b]Bold numbers indicate a significant expansion according to the criteria described in Materials and methods.

spectratyping. This technique allows us to assess the clonal composition of a T cell population and its overall diversity based on the length of TCRB CDR3 (18, 19). For CD4$^+$ cells (12 samples analyzed), in every instance a full CDR3 length diversity was restored at 2 yr of follow-up, both when CDR3 distribution at baseline was skewed (Fig. 4 A and not depicted) and when it was normally diverse (Fig. 4 B and not depicted). In the CD8$^+$ subset (72 samples), TCRBV expansions appearing at 6 mo or 1 yr after HCST were usually associated with a skewed, oligo-, or monoclonal CDR3-length distribution (Fig. 4, A and C, and not depicted). Some CDR3 peaks that were dominant at baseline reemerged at follow-up, indicating that oligoclonal T cells that had rearranged the same TCRBV gene and a CDR3 of equal length either persisted or were selected and expanded again after HSCT (Fig. 4 C). In six out of seven patients, both for the CD4 and for CD8 subsets, we observed almost exclusively the first two patterns presented in Fig. 4 (i.e., increased or preserved diversity). In patient 5, we frequently observed the reappearance posttherapy of CD8$^+$ T cells with the same CDR3 length. Interestingly, this was the only patient who had recurrent infectious events during follow-up and the only patient who had a substantial loss of CD8 TREC posttherapy. However, even when we found a skewed CDR3-length distribution posttherapy, the CDR3 peaks that were dominant pretherapy became subdominant posttransplant, outnumbered by others that were underrepresented or undetectable before therapy (Fig. 4 C and not depicted). Overall, normal CDR3 length distribution was reconstituted for the majority of the TCR repertoires, suggesting increased clonal diversity from de novo TCR rearrangement.

Extensive clonal T cell renewal after HSCT

To examine a section of the TCR repertoire at the single clone level, we cloned and sequenced TCRB transcripts from sorted peripheral blood CD4$^+$ and CD8$^+$ T cells ob-
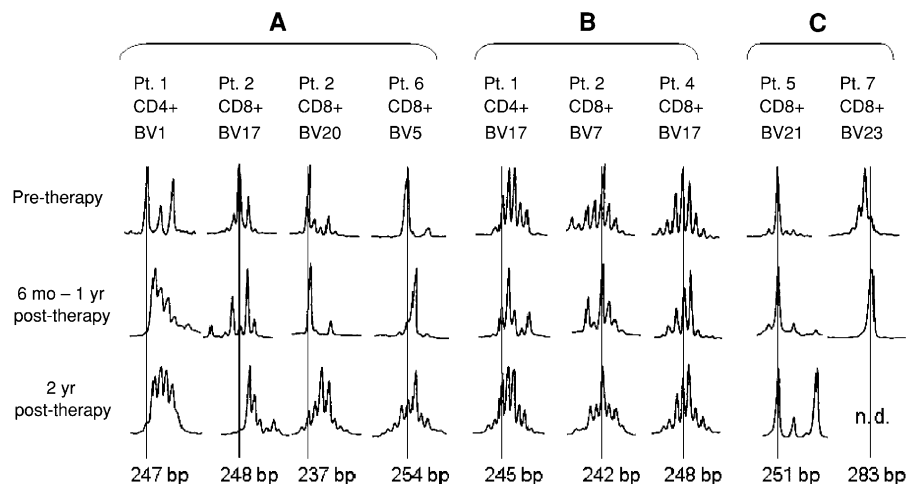
Figure 4. Analysis of TCR diversity. High-resolution TCRBV CDR3 spectratyping analysis identified three basic patterns of evolution of repertoire diversity: (A) recovery of diversity from a restricted repertoire, (B) reconstitution of diversity from a normally diverse repertoire; (C) and total or partial persistence (or reemergence) of repertoire skewing. Different numbers of examples are shown to convey a correct impression of the observed frequency of each pattern. Patterns A and B were largely predominant except for patient 5, who had recurrent infections. Vertical lines are reference DNA size markers to provide the exact correspondence of CDR3 peaks across different samples. n.d., not determined (due to unavailability of 2-yr follow-up for patient 7).

tained at baseline and posttreatment. We selected 10 sample pairs (preTx and corresponding 1-yr or 2-yr follow-up) covering the three different patterns of reconstitution of TCR repertoire diversity observed by CDR3-length spectratyping and sequenced 90 clones on both DNA strands for each sample (patient/time point/T subset/BV gene). Representative results of sequencing-based clonotypic analysis for each of the three categories are shown in Fig. 5. When CDR3-length diversity was increased or maintained (spectratyping patterns A and B, respectively), we observed a very substantial or complete renewal of the clonal specificities. New sequences represented from 90 to 100% of the examined portion of T cell repertoire (Fig. 5, A and B, and not depicted). For sample pairs with spectratyping pattern A, the vast majority of the new sequences in the posttherapy T repertoire fraction examined were unique clones (appearing only once), consistent with the notion of increased repertoire diversity (Fig. 5 A and not depicted). Surprisingly, the proportion of unique sequences increased posttherapy also for sample pairs that had a spectratyping pattern B (Fig. 5 B and not depicted), demonstrating an increased diversity of individual clones within each CDR3 length (i.e., within each spectratyping peak). In the fewer observed instances of limited CDR3-length diversity posttherapy (pattern C), the proportion of unique sequences was reduced, as expected. The frequency of expanded clones (same TCR sequence appearing more than once) was always decreased posttherapy in patterns A and B (Fig. 5, A and B, and not depicted). In contrast, for pattern C, the total frequency of expanded clones was increased posttherapy. However, the hierarchy of frequency of preexisting individual clones was often reversed posttherapy (i.e., dominant clones became subdominant and vice versa). In addition, to our surprise, newly appearing

clones (both expanded and not expanded) represented up to 100% of all TCRBV gene family transcripts in posttreatment samples with limited clonal diversity, indicating that clonally expanded populations could originate to a large extent or even entirely from de novo–selected T cells (Fig. 5 C and not depicted). The extent of clonal renewal, defined as the percentage of new sequences posttherapy (including both nonexpanded and expanded clones) ranged from 89.4 to 100% for group A, from 90.4 to 100% for group B, and from 12 to 100% for group C.

Effects on peripheral aspects of immune reconstitution

Because peripheral mechanisms of immune homeostasis during and after immune reconstitution may also contribute to the remission of inflammatory disease activity, we examined by flow cytometry immunological markers of cell activation, costimulation, adhesion, chemotaxis, and apoptotic pathways on T cells, B cells, monocytes, and T cell subsets. Among the most significant changes we observed a prominent increase in the frequency of CD95/Fas$^+$ T cells at 6 mo posttransplant ($P < 0.002$ for the CD8$^+$ subset), suggesting an increased susceptibility to Fas/FasL–mediated apoptosis (Fig. 6 A). We focused further analyses on the CD8$^+$ subset because previous papers (9, 10) and our emerging data suggested a major contribution of CD8$^+$ T cells to the peripheral (postthymic) component of immune reconstitution. After HSCT, a larger proportion of CD8$^+$ cells lacked CD28 expression and expressed CD57 ($P < 0.001$ at all time-points posttherapy compared with baseline; Fig. 6 B). CD8$^+$/CD28$^-$/CD57$^+$ T cells have been described recently as a subpopulation that is unable to expand upon stimulation and is highly susceptible to apoptosis (20). Considering the aforementioned oligoclonal T cell expansions in the CD8$^+$ subset after HSCT, we
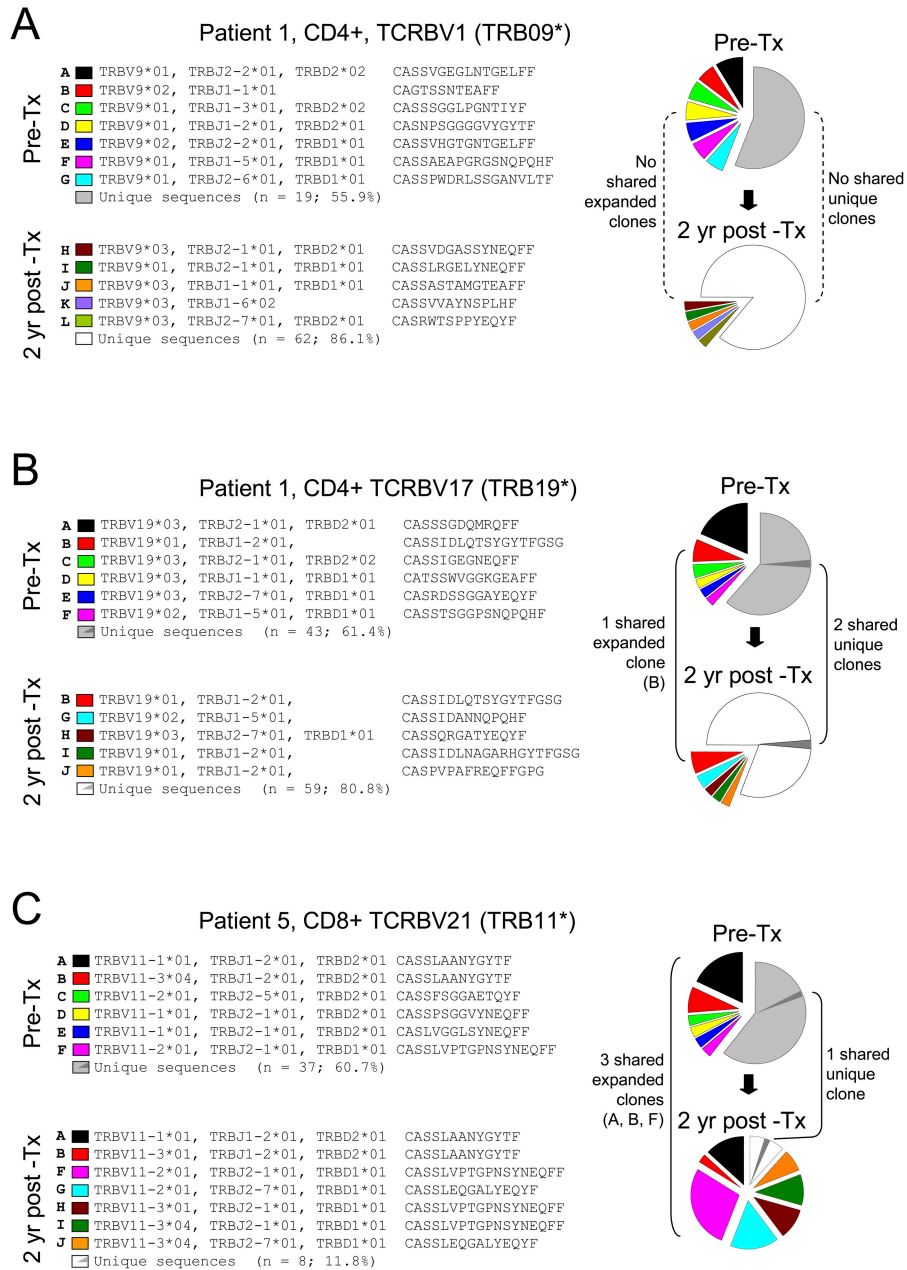
A   Patient 1, CD4+, TCRBV1 (TRB09*)

Pre-Tx
A	■	TRBV9*01, TRBJ2-2*01, TRBD2*02 CASSVGEGLNTGELFF
B	■	TRBV9*02, TRBJ1-1*01 CAGTSSNTEAFF
C	■	TRBV9*01, TRBJ1-3*01, TRBD2*02 CASSSGGLPGNTIYF
D	■	TRBV9*01, TRBJ1-2*01, TRBD2*01 CASNPSGGGGVYGYTF
E	■	TRBV9*02, TRBJ2-2*01, TRBD1*01 CASSVHGTGNTGELFF
F	■	TRBV9*01, TRBJ1-5*01, TRBD1*01 CASSAEAPGRGSNQPQHF
G	■	TRBV9*01, TRBJ2-6*01, TRBD1*01 CASSPWDRLSSGANVLTF
	▨	Unique sequences (n = 19; 55.9%)

2 yr post -Tx
H	■	TRBV9*03, TRBJ2-1*01, TRBD2*01 CASSVDGASSYNEQFF
I	■	TRBV9*01, TRBJ2-1*01, TRBD1*01 CASSLRGELYNEQFF
J	■	TRBV9*03, TRBJ1-1*01, TRBD1*01 CASSASTAMGTEAFF
K	■	TRBV9*03, TRBJ1-6*02 CASSVVAYNSPLHF
L	■	TRBV9*03, TRBJ2-7*01, TRBD2*01 CASRWTSPPYEQYF
	☐	Unique sequences (n = 62; 86.1%)

B   Patient 1, CD4+ TCRBV17 (TRB19*)

Pre-Tx
A	■	TRBV19*03, TRBJ2-1*01, TRBD2*01 CASSSGDQMRQFF
B	■	TRBV19*01, TRBJ1-2*01, CASSIDLQTSYGYTFGSG
C	■	TRBV19*03, TRBJ2-1*01, TRBD2*02 CASSIGEGNEQFF
D	■	TRBV19*03, TRBJ1-1*01, TRBD1*01 CATSSWVGGKGEAFF
E	■	TRBV19*03, TRBJ2-7*01, TRBD1*01 CASRDSSGGAYEQYF
F	■	TRBV19*02, TRBJ1-5*01, TRBD1*01 CASSTSGGPSNQPQHF
	▨	Unique sequences (n = 43; 61.4%)

2 yr post -Tx
B	■	TRBV19*01, TRBJ1-2*01, CASSIDLQTSYGYTFGSG
G	■	TRBV19*02, TRBJ1-5*01, CASSIDANNQPQHF
H	■	TRBV19*03, TRBJ2-7*01, TRBD1*01 CASSQRGATYEQYF
I	■	TRBV19*01, TRBJ1-2*01, CASSIDLNAGARHGYTFGSG
J	■	TRBV19*01, TRBJ1-2*01, CASPVPAFREQFFGPG
	☐	Unique sequences (n = 59; 80.8%)

C   Patient 5, CD8+ TCRBV21 (TRB11*)

Pre-Tx
A	■	TRBV11-1*01, TRBJ1-2*01, TRBD2*01 CASSLAANYGYTF
B	■	TRBV11-3*04, TRBJ1-2*01, TRBD2*01 CASSLAANYGYTF
C	■	TRBV11-2*01, TRBJ2-5*01, TRBD2*01 CASSFSGGAETQYF
D	■	TRBV11-1*01, TRBJ2-1*01, TRBD2*01 CASSPSGGVYNEQFF
E	■	TRBV11-1*01, TRBJ2-1*01, TRBD2*01 CASLVGGLSYNEQFF
F	■	TRBV11-2*01, TRBJ2-1*01, TRBD1*01 CASSLVPTGPNSYNEQFF
	▨	Unique sequences (n = 37; 60.7%)

2 yr post -Tx
A	■	TRBV11-1*01, TRBJ1-2*01, TRBD2*01 CASSLAANYGYTF
B	■	TRBV11-3*01, TRBJ1-2*01, TRBD2*01 CASSLAANYGYTF
F	■	TRBV11-2*01, TRBJ2-1*01, TRBD1*01 CASSLVPTGPNSYNEQFF
G	■	TRBV11-2*01, TRBJ2-7*01, TRBD1*01 CASSLEQGALYEQYF
H	■	TRBV11-3*01, TRBJ2-1*01, TRBD1*01 CASSLVPTGPNSYNEQFF
I	■	TRBV11-3*04, TRBJ2-1*01, TRBD1*01 CASSLVPTGPNSYNEQFF
J	■	TRBV11-3*04, TRBJ2-7*01, TRBD1*01 CASSLEQGALYEQYF
	☐	Unique sequences (n = 8; 11.8%)

Figure 5. **Extensive clonotypic renewal within the T cell repertoire.** We cloned and sequenced 90 clonal TCRs from sample pairs for each of the three patterns of evolution of CDR3 length diversity previously identified by spectratyping. One representative example is shown for each pattern. Colored pie slices represent individual expanded T clones. Color and size of slices allow identification of the expanded clones and show their relative frequency, respectively. The group of nonexpanded clones (unique sequences, not shown individually for their large numbers) is shown in light gray in pretransplant samples and in white in posttransplant samples and, within each one, the proportion of single clones persisting posttransplantation is shown in dark gray. For the predominant patterns in A and B, we found a prominent increase of unique sequences, denoting increased clonal diversity also within the same CDR3 length. Pre-existing expanded clones were either undetectable or reduced after therapy. In the less frequent pattern in C, preexisting or new expanded clones constituted the majority of the examined T repertoire after therapy.

investigated the nature of these expansions with relevant cell surface markers, alone or in combination with specific TCR Vβ staining (Fig. 7, A and B). The examination of oligoclonal T cell expansions based on back-gating on the expressed TCR Vβ (Fig. 7 B) showed that >95% of the expanded TCR Vβ–bearing cells was CD57+ (Fig. 7 C).

Further characterization described these cells as CD95/Fas+, CD45RA+/CD45RO+/CD27− atypical effector–memory CD8+ T cells (Fig. 7 C). Because CD8+/CD57+/CD28− T cells represent a state of proliferative senescence reached after extensive division in vivo and loss of TRECs (20), their expansion after HSCT accounted for the lack of increase (or
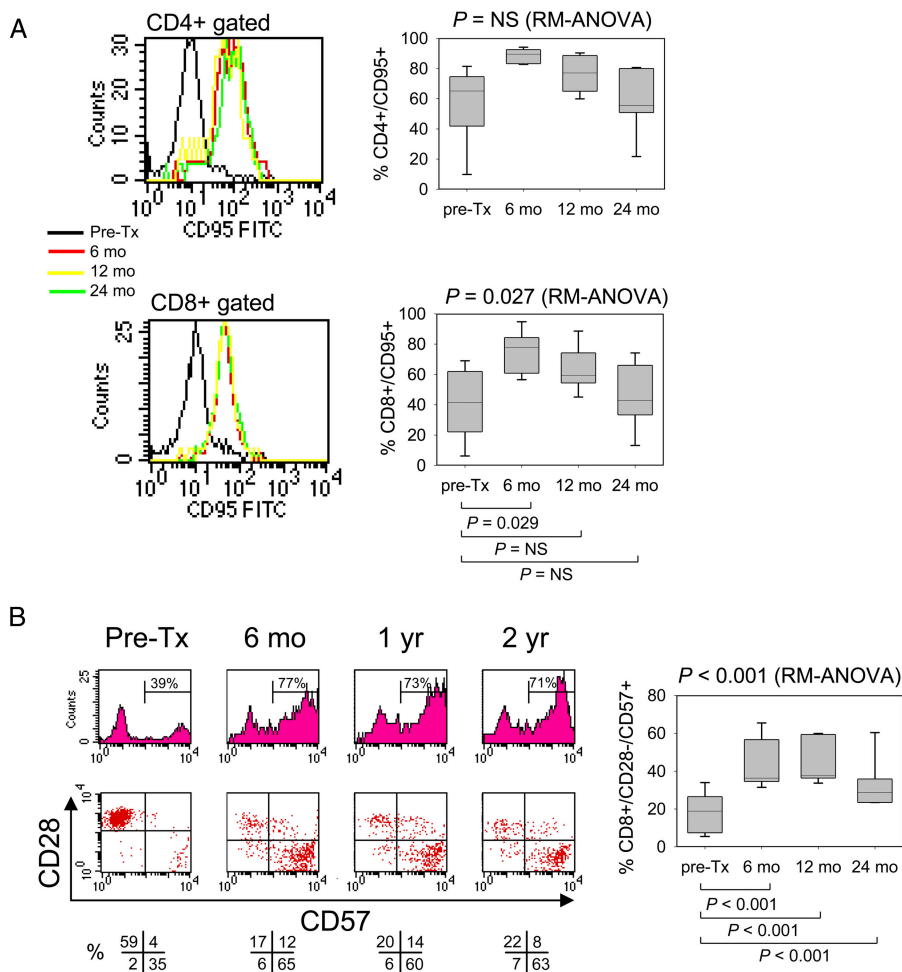
Figure 6. Phenotypic changes of the peripheral T cell repertoire. (A) Transient increase of CD95/Fas^{+} in the CD4^{+} and CD8^{+} T cell subset in the early (peripheral) phases of immune reconstitution, suggesting an increased susceptibility to Fas/FasL-mediated apoptosis. Representative histograms from an individual patient are shown (left) as is a summary of data from all patients (right). (B) Persistent increase of CD8^{+}/CD28^{−}/CD57^{+} T cells during follow-up. (left) An individual patient's example of CD8^{+} gated analysis with the top histograms showing CD57 expression, and dot plots (bottom) showing CD57 (x axis) versus CD28 (y axis) expression. (right) The box plot summarizes the data from all patients. CD8^{+}/CD28^{−}/CD57^{+} have been characterized as a terminally differentiated subpopulation with short telomeres, defective cytolytic functions, and increased susceptibility to apoptosis.

loss) of CD8 TRECs posttherapy in the individuals with more prominent or persistent TCR Vβ expansions in the CD8^{+} subset (patient nos. 2, 5, and 7).

DISCUSSION

MS is an inflammatory disease believed to have a T cell–mediated autoimmune origin. To understand the capacity of T cells to regenerate after autologous HSCT in patients with MS, we focused on the long-term posttherapy reconstitution of the T cell immune compartment. The main question we wanted to address was whether the favorable effects of HSCT on the inflammatory component of disease are related to a "resetting" of the adaptive immune system, as often postulated, or are simply the result of a long-lasting lymphocyte depletion induced by the high–dose immunoablative therapy. Because, in our work, the recovery of leuko-

cyte and T cell subset absolute numbers was not associated with reemergence of inflammatory disease activity, other changes in the immune systems must be considered to explain the observed disease relapse-free interval for the entire 2-yr posttherapy follow-up.

Our data show that a thymopoietic pathway of T cell regeneration is activated in MS patients treated with HSCT and leads to immune renewal. The evidence supporting this notion is as follows: (a) the increased frequency of phenotypically naive CD4^{+} T cells; (b) the decreased frequency of central–memory T cells; (c) the expansion of phenotypically identified CD4^{+} RTEs; (d) the increased TREC levels in the CD4^{+} subset and the adequate recovery of CD8 TRECs in spite of extensive peripheral division in this subset; (e) the overall improved clonal diversity of the TCR repertoire; and (f) the extensive clonotypic renewal shown
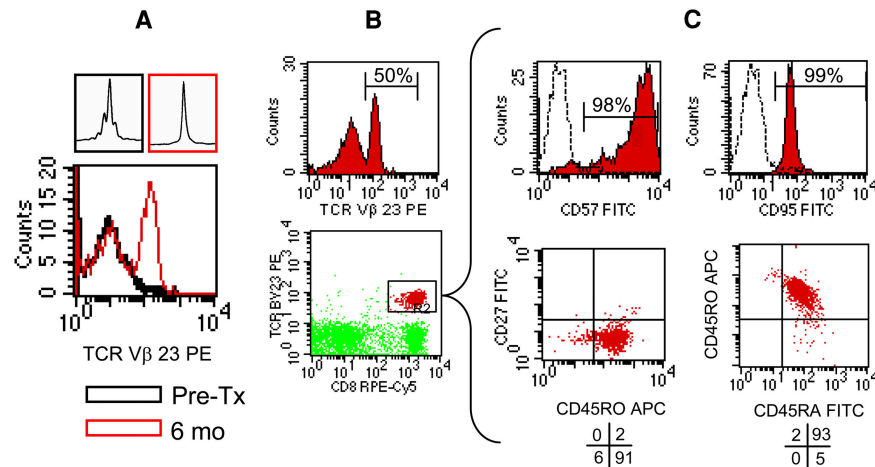
Figure 7. Characterization of oligoclonally expanded CD8$^+$ populations. (A) In the example shown, TCR Vβ back-gating in combination with CDR3 spectratyping of CD8$^+$ T cells (top inlays: black box, preHSCT; red box, 6-mo follow-up) demonstrates that oligoclonal expanded cells, representing up to 50% of all CD8$^+$ cells (B), are CD57$^+$/CD45RA$^+$/CD45RO$^+$/CD27$^-$/CD95(Fas)$^+$ (C), consistent with the phenotype of atypical effector–memory cells that reached replicative senescence after extensive division in vivo.

by comparison of pre- and posttherapy TCRBV transcripts. Thymus-dependent T cell regeneration is more vigorous in the early childhood (21), but recent data have shown that the thymus is still active through adult life (22). However, patients with MS have age-inappropriate TREC levels, suggesting an intrinsic impairment of thymic export (23). A major finding of our study is the simultaneous reemergence posttherapy of phenotypically naive CD4$^+$ cells and CD4$^+$ RTEs, which led to a doubling of their frequency at 2 yr posttransplantation compared with pretherapy. This observation suggests that increased thymopoiesis ("thymic rebound") after HSCT can correct the preexisting deficiency and normalize naive T cell homeostasis. Recent studies in animal models have shown that reconstitution of the thymus by hematopoietic stem cells, rather than peripheral homeostasis, determines peripheral naive CD4$^+$ T cell reconstitution (24). Irradiation of the host was required for accumulation of naive T cells (24, 25). Whether total body irradiation (TBI), used in our treatment regimen, is also a requirement in humans for the induction of naive cell expansion remains to be determined. The reciprocal decrease of central–memory T cells we observed is intriguing in the context of MS because this subset represents the major component of cerebrospinal fluid T cells (12), and memory cells are more easily triggered and more cross–reactive than naive cells. The overall increased diversity of TCRB CDR3-length repertoire is also consistent with increased thymic output (11). The aforementioned observations contrast with available data from conventional chemotherapy for MS, including pulse cyclophosphamide and mitoxantrone, which both lead to decreased CD4$^+$ total and naive cell numbers, arguing for immunosuppressive effects rather than for immune renewal (26, 27).

Using a sequencing-based clonotypic analysis, we explored for the first time at the single clone level the reconstitution of TCR repertoire after HSCT in an immune-mediated disease. Two important observations emerged from our data; first, the extent of T cell repertoire renewal is even greater (>90% in most cases) than what could be anticipated from the increase of naive cells and of RTEs or from the reconstitution of CDR3 length diversity that we have observed. Second, although the renewal of clonal specificities is extensive, it is not always complete, and some preexisting individual T cell clones, more frequently in the CD8$^+$ subset, can be found again in the peripheral blood after HSCT. To understand the origin of the persisting clones, we are attempting to track them in the minor T cell component contaminating the CD34$^+$ enriched hematopoietic stem cell graft. The relevance for disease of these clones remains unclear. In fact, their persistence in subjects showing a sustained remission of inflammatory disease activity suggests that either these clones were not self-reactive pathogenic mediators or they are not able to induce disease activity under the new conditions produced by the immune reconstitution.

Early thymus–independent pathways dictate a faster numeric regeneration of CD8$^+$ T cells than for CD4$^+$ cells, and the observation of clonal expansions in the CD8$^+$ subset suggests a role of antigen-specific differentiated cells in its repopulation. Our data show that oligoclonal cells are a major constituent of the expansion of CD8$^+$/CD28$^-$/CD57$^+$ T cells. Because of their ambiguous phenotype and the coexpression of high and low molecular weight CD45R isoforms, these cells cannot be reliably classified as central– or effector–memory cells according to conventional schemes. Extensive peripheral cell division in the CD8$^+$ subset reduces TREC content and probably masks an underlying increase from thymic rebound, leading to an underestimate of the frequency of naive CD8$^+$ and CD8 RTEs as suggested previously (11). The activation of similar cell populations in recipients of HSCT has been correlated to previous expo-

sure to CMV (9, 28), leading to the notion that CD28$^-$/CD57$^+$ cells are differentiated memory CD8$^+$ populations expanded in the presence of persistent viral antigens. CD8$^+$/CD28$^-$/CD57$^+$ T cells have limited TCR diversity also in healthy subjects (29, 30), have short telomeres (20, 31), are unable to proliferate in vitro, and are highly susceptible to apoptosis (20). Consistent with the latter observation, the elevated frequency of Fas$^+$CD8$^+$ (and CD4$^+$) cells that we and others found in the early phases of immune reconstitution has been linked to a generally increased propensity to apoptosis (32, 33). Based on all these characteristics, the CD8$^+$/CD28/CD57$^+$ phenotype has been viewed as a signature of "clonal exhaustion" or "replicative senescence" (20, 34, 35). The expansion of atypical, terminally differentiated CD8$^+$ cells may be implied in the control of autoimmunity by restricting the space available in the effector–memory niche for other cells, possibly including autoreactive effectors, through a process known as attrition (13, 36). In addition, CD8$^+$/CD28$^-$/CD57$^+$ T cells can exert an immunoregulatory role mediated via an unidentified soluble factor (37–39).

Further studies are required to better understand the mechanisms that underlie these observations and their possible implications for immune tolerance. Here, we showed that a sequential combination of thymus-independent peripheral reconstitution pathways (early; CD8 > CD4) and thymus-dependent immune rejuvenation (later; CD4 > CD8) profoundly reconfigures the immune system in patients with MS who received HSCT and results in a prolonged disease activity–free interval that is not reliant on immunosuppression. These findings substantiate the induction of immune regeneration as the rationale of HSCT and provide a mechanistic basis for ongoing and future clinical trials of this therapeutic strategy in autoimmune diseases.

MATERIALS AND METHODS

Clinical trial protocol. Enrollment in the protocol required a diagnosis of clinically definite MS (40) and a neurological progression during the year before screening evaluation of at least 1.5 steps on the expanded disability status scale (EDSS; a measure of disability ranging from 0 for a normal neurologic exam to 10 for death as a result of MS; reference 41) if their initial grade was 6.0 or less, or at least 1.0 step if their EDSS at screening was ≥6.5. Additional inclusion criteria required that baseline EDSS levels had to be sustained for at least 3 mo and unresponsive to high dose steroid treatment. The study was approved by the U.S. Food and Drug Administration under IDE 6440 and by the institutional review boards of Northwestern University and of the National Institute of Neurological Disorders and Stroke, National Institutes of Health. Seven patients with MS (Table I) gave informed consent and were consecutively enrolled in the study. Peripheral blood stem cells were collected by leukapheresis after infusion of 2.0 g/m^2 cyclophosphamide followed by daily G-CSF (5 μg/kg/d) beginning 72 h after cyclophosphamide infusion. The graft was enriched for CD34$^+$ cells by Isolex (Baxter) stem cell concentrator. Data on the purity of the CD34$^+$ enriched hematopoietic stem cell grafts are reported in Table III. Immune ablation was achieved by 60 mg/kg/d cyclophosphamide intravenously for 2 d, followed by TBI in doses of 150 cGy, twice daily, for a consecutive 4 d (total dosage of 1,200 cGy). 1 g methylprednisolone was administered intravenously on each of the 4 d of TBI. Further details of the clinical trial have been published (42).

Clinical responses to HSCT. All seven patients successfully completed the protocol treatment. There were no transplant-related toxicities during follow-up. Patient 5 had recurrent episodes of *Clostridium difficile* enterocolitis after HSCT. No infectious events were observed in the other six patients during follow-up. All patients remained free of clinical MS relapses after HSCT for a mean follow-up of 27.6 mo (range: 21–36 mo) without receiving any immunosuppressive or –modulatory treatment (Table I). Magnetic resonance imaging (MRI) of the brain (and of the spinal cord for four patients) performed at 6 mo after HSCT and yearly thereafter showed an absence of gadolinium-enhancing lesions for a mean follow-up of 30 mo (range: 24–36 mo) as exemplified in Fig. 1. Clinical disability at 2-yr follow-up improved in one patient (from EDSS 3.5 to 1.0) and remained stable (variation of EDSS ≤ 0.5) in five patients. One patient (no. 7) who had progressively worsened by 1.0 EDSS point at 1 yr after HSCT was lost to follow-up because of accidental injuries at 21 mo after HSCT. During the

Table III. Purity of the CD34$^+$ enriched hematopoietic stem cell grafts

Patient	Graft no.[a]	Volume	Percent CD34$^+$/ml	No. of CD34$^+$/ml	Total CD34$^+$ infused[b]	Percent CD3$^+$	No. of CD3$^+$/ml	Total CD3$^+$ infused[b]
		ml						
1	1	101	92.0	2.21×10^6	4.07×10^8	0.10	2.40×10^3	8.54×10^5
	2	102	90.4	1.81×10^6		0.30	6.00×10^3	
2	1	102	96.3	5.49×10^6	5.60×10^8	0.20	1.14×10^4	1.16×10^6
3	1	102	93.5	4.39×10^6	4.48×10^8	0.10	4.70×10^3	4.79×10^5
4	1	103	71.8	4.88×10^6	5.03×10^8	0.10	6.80×10^3	7.00×10^5
5	1	101	92.7	3.24×10^6	3.28×10^8	0.10	3.50×10^3	3.53×10^5
6	1	103	70.4	1.83×10^6	1.89×10^8	0.60	1.56×10^4	1.61×10^6
7	1	102	63.3	1.20×10^6	2.81×10^8	0.60	1.14×10^4	1.37×10^6
	2	102	77.7	1.55×10^6		0.10	2.00×10^3	
Average		102	83.1	2.96×10^6	3.88×10^8	0.24	7.09×10^3	9.32×10^5

[a]For patients 1 and 7, the number of mobilized CD34$^+$ obtained from the first leukapheresis was insufficient; therefore, a second collection was performed the following day.
[b]For patients 1 and 7, we indicate the total combined number of CD34$^+$ and CD3$^+$ cells calculated from graft nos. 1 and 2 that were infused into the patient. The purity of each graft is reported separately.

available posttherapy follow-up, this patient had no clinical relapses or MRI evidence of disease activity. Therefore, chronic progression of disability was probably consequent to axonal degenerative processes that may occur in progressive stages of disease even in the absence of inflammation (42–44). For the purposes of this study, the absence of exacerbations and absence of active or new lesions posttherapy after HSCT in all patients indicated a profound effect on the inflammatory component of MS pathogenesis, consistent with other reports (45–47).

Cells and immunophenotypic analyses. Routine complete blood counts and differential white blood cell counts were obtained at study visits. PBMCs were collected at baseline before stem cell mobilization and at 6, 12, and 24 mo posttransplant and were isolated and cryopreserved according to standard methods. We examined the expression of a large panel of cell surface markers on T cells, B cells, monocytes, and T cell subsets using four-color FACS analysis. The markers included molecules crucially involved in T cell activation, costimulation, chemotaxis, apoptosis, adhesion, and transmigration as well as markers of specialized T cell subpopulations. A total of 24 different mAb combinations allowed the acquisition and analysis of a minimum of 98 immunological measures for each PBMC sample. The following antibodies were purchased from BD Biosciences: CD3 Cy-Chrome, CD8 FITC, CD8 PE, CD14 allophycocyanin, CD14 FITC, CD14 PE, CD31 PE, CD19 FITC, CD28 PE, CD40 FITC, CD40 Cy-Chrome, CD45RA FITC, CD45RO PE, CD45RO allophycocyanin, CD49d FITC, CD54 (ICAM-1) PE, CD56 PE, CD58 (LFA-3) FITC, CD69 FITC, CD74 FITC, CCR4 PE, CCR5 PE, CXCR3 PE, CXCR4 PE (BD), CD134 (OX-40) FITC, CD134 (OX-40) FITC, CD152 (CTLA-4) PE, CD154 (CD40L) PE, CD80 PE, CD86 FITC, CD95 PE, HLA-DQ FITC, HLA-DR FITC, HLA-DR Cy-Chrome, TCR α/β FITC, TCR γ/δ PE, IgG1 Cy-Chrome, IgG2a κ PE, IgG2a κ FITC, IgG2b κ FITC, and IgG2b κ PE. We purchased the following antibodies from Exalpha: CD4 FITC, CD4 RPE-Cy5, CD8 allophycocyanin, CD19 FITC, CD25 FITC, CD27 FITC, CD45RA PE, CD69 FITC, CD117 (C-KIT L) FITC, IgG1 FITC, IgG1 PE, IgG1 RPE-Cy5, IgG1 allophycocyanin, and IgG2a κ allophycocyanin. The antibodies CD45RO FITC and CD83 PE were obtained from Beckman Coulter. CCR1 PE, CCR2 PE, CCR3 FITC, and CCR5 FITC were obtained from R&D Systems.

Stringent control of antibody lot consistency, staining conditions, and instrument setup allowed excellent interexperimental reproducibility (unpublished data).

Measurement of thymic output. Frequency of RTEs in peripheral blood was evaluated by quantitative PCR for detection of TRECs as described previously (22). In brief, we purified CD4$^+$ and CD8$^+$ T cell subsets using MACS microbeads (Miltenyi Biotec). Sorted cells (>95% pure by FACS analysis) were counted and lysed with proteinase K, and the exposed DNA was used directly as template for real-time quantitative PCR amplification and quantification. Real-time PCR was run in duplicate tubes, and a standard curve was generated from a plasmid TREC DNA serial dilution (six concentrations), allowing absolute TREC quantification and accurate measuring of TREC per unit number of cells.

Analysis of TCR repertoire. We performed an analysis of TCR Vβ expression on peripheral blood CD4$^+$ and CD8$^+$ T cells by four-color FACS analysis using 22 TCR Vβ–specific monoclonal antibodies as described previously (48). TCR designations are according to Arden's nomenclature (49). A TCR Vβ was defined significantly expanded at follow-up when its percent expression met all three of the following criteria: (a) exceeding by at least 2 SD the mean expression in a reference population of 64 healthy donors (48); (b) being at least twice the baseline expression in that individual; and (c) being ≥5% of all TCR Vβ$^+$ cells.

To analyze the clonal heterogeneity of TCRBV gene rearrangements by CDR3 spectratyping, CD4$^+$ and/or CD8$^+$ T cell subsets were positively selected using MACS (Miltenyi Biotec). Purity of sorted subsets was >95%. RNA was isolated using TRIzol (Invitrogen) and complementary DNA (cDNA) was synthesized using SuperScript II and Oligo-dT (both obtained from Invitrogen) according to the manufacturer's instructions. TCRB rearrangements were amplified from cDNA using BV family–specific oligonucleotide primers essentially as described previously (48) and 2.5 μl of PCR amplification product from each TCR BV were used as template in a 12.5 μl primer-extension ("runoff") reaction containing 1.25 μl of 5′ FAM-labeled BV primer, 0.25 μl of 10 mM dNTP (Invitrogen), 0.06 μl PFU DNA polymerase (Promega), 1.25 μl PFU reaction buffer, and 7.2 μl H$_2$O. After thermal cycling (95°C for 2 min; followed by 10 cycles of 94°C for 20 s, 55°C for 45 s, and 72°C for 45 s, and a final extension of 72°C for 10 min), 2 μl of runoff reaction product was mixed with a loading buffer containing four Cy-5–labeled DNA-size markers (sizes 103, 152, 205, and 261 bp), heat treated at 80°C for 2 min, and run on a 6% polyacrylamide gel on an OpenGene (Visible Genetics) sequencer. Electropherograms were analyzed using the OpenGene software package. Analysis included peak size (expressed in base pairs), peak height, and area under the curve (AUC). For evaluation of normal (Gaussian) versus skewed (oligoclonal) CDR3-length distribution, the percentage represented by each CDR3 peak in a BV spectrum (corresponding to the representation of clonal populations with a given CDR3 length) was calculated according to the formula %AUC BVn = (AUC BVn / ΣAUC all BV) × 100.

For TCR β–chain sequencing, TCRBV rearrangements were amplified from CD4$^+$ or CD8$^+$ sorted cells essentially as described before, and amplicons were purified by agarose gel electrophoresis using the Gel Extraction Kit (QIAGEN). The purified DNA fragments were ligated into a pGEM-T Easy vector (Promega) and were used to transform DH5α *Escherichia coli* (Invitrogen) competent cells. For each TCRBV 90, individual bacterial colonies were selected by blue/white screening, and plasmid DNA was extracted using standard methods. Samples were sequenced on an ABI 373 automated sequencing system. Dye-labeled vector-specific primers (T7-forward and Sp6-reverse) were used to sequence both strands of each clone. Sequence analysis was completed with the Genetics Computer Group–Lite Software, and TCR rearrangements were analyzed using IMGT, the international ImMunoGeneTics information system at http://imgt.cines.fr.

Statistical analysis. The statistical significance of immunological changes was longitudinally evaluated by one-way repeated measures analysis of variance (RM-ANOVA). When RM-ANOVA identified a statistically significant change, the Tukey post-hoc test was applied. When appropriate, the paired Student's *t* test or the nonparametric Mann–Whitney rank sum test was applied. To test for correlation of normally distributed variables, we used Pearson's correlation coefficient.

Online supplemental material. Fig. S1 exemplifies an analysis of TCR Vβ expression for the CD4 and the CD8 subsets during a 2-yr follow-up and the detection of a significant T cell expansion in the CD8 subset. Fig. S2 depicts a multidimensional scaling analysis of the extent of similarity of the reconstituting TCR Vβ profiles for the CD4 and CD8 T cell subsets of each patient. Online supplemental material is available at http://www.jem.org/cgi/content/full/jem.20041679/DC1.

REFERENCES

1. Hafler, D.A. 2004. Multiple sclerosis. *J. Clin. Invest.* 113:788–794.
2. Muraro, P.A., R. Cassiani Ingoni, and R. Martin. 2003. Hematopoietic stem cell transplantation for multiple sclerosis: current status and future challenges. *Curr. Opin. Neurol.* 16:299–305.

3. Fassas, A., and V.K. Kimiskidis. 2003. Stem cell transplantation for multiple sclerosis: what is the evidence? *Blood Rev*. 17:233–240.

4. Burt, R.K., S. Slavin, W.H. Burns, and A.M. Marmont. 2002. Induction of tolerance in autoimmune diseases by hematopoietic stem cell transplantation: getting closer to a cure? *Blood*. 99:768–784.

5. Fassas, A., A. Anagnostopoulos, A. Kazis, K. Kapinas, I. Sakellari, V. Kimiskidis, and A. Tsompanakou. 1997. Peripheral blood stem cell transplantation in the treatment of progressive multiple sclerosis: first results of a pilot study. *Bone Marrow Transplant*. 20:631–638.

6. Burt, R.K., A.E. Traynor, B. Cohen, K.H. Karlin, F.A. Davis, D. Stefoski, C. Terry, L. Lobeck, E.J. Russell, C. Goolsby, et al. 1998. T cell–depleted autologous hematopoietic stem cell transplantation for multiple sclerosis: report on the first three patients. *Bone Marrow Transplant*. 21:537–541.

7. Openshaw, H., B.T. Lund, A. Kashyap, R. Atkinson, I. Sniecinski, L.P. Weiner, and S. Forman. 2000. Peripheral blood stem cell transplantation in multiple sclerosis with busulfan and cyclophosphamide conditioning: report of toxicity and immunological monitoring. *Biol. Blood Marrow Transplant*. 6:563–575.

8. Sun, W., U. Popat, G. Hutton, Y.C. Zang, R. Krance, G. Carrum, G.A. Land, H. Heslop, M. Brenner, and J.Z. Zhang. 2004. Characteristics of T-cell receptor repertoire and myelin-reactive T cells reconstituted from autologous haematopoietic stem-cell grafts in multiple sclerosis. *Brain*. 127:996–1008.

9. Reimer, P., V. Kunzmann, M. Wilhelm, B. Weissbrich, D. Kraemer, H. Berghammer, and F. Weissinger. 2003. Cellular and humoral immune reconstitution after autologous peripheral blood stem cell transplantation (PBSCT). *Ann. Hematol*. 82:263–270.

10. Koehne, G., W. Zeller, M. Stockschlaeder, and A.R. Zander. 1997. Phenotype of lymphocyte subsets after autologous peripheral blood stem cell transplantation. *Bone Marrow Transplant*. 19:149–156.

11. Berzins, S.P., A.P. Uldrich, J.S. Sutherland, J. Gill, J.F. Miller, D.I. Godfrey, and R.L. Boyd. 2002. Thymic regeneration: teaching an old immune system new tricks. *Trends Mol. Med*. 8:469–476.

12. Kivisakk, P., D.J. Mahad, M.K. Callahan, C. Trebst, B. Tucky, T. Wei, L. Wu, E.S. Baekkevold, H. Lassmann, S.M. Staugaitis, et al. 2003. Human cerebrospinal fluid central memory CD4+ T cells: evidence for trafficking through choroid plexus and meninges via P-selectin. *Proc. Natl. Acad. Sci. USA*. 100:8389–8394.

13. Jameson, S.C. 2002. Maintaining the norm: T-cell homeostasis. *Nat. Rev. Immunol*. 2:547–556.

14. Murali-Krishna, K., and R. Ahmed. 2000. Cutting edge: naive T cells masquerading as memory cells. *J. Immunol*. 165:1733–1737.

15. Goldrath, A.W., L.Y. Bogatzki, and M.J. Bevan. 2000. Naive T cells transiently acquire a memory-like phenotype during homeostasis-driven proliferation. *J. Exp. Med*. 192:557–564.

16. Kimmig, S., G.K. Przybylski, C.A. Schmidt, K. Laurisch, B. Mowes, A. Radbruch, and A. Thiel. 2002. Two subsets of naive T helper cells with distinct T cell receptor excision circle content in human adult peripheral blood. *J. Exp. Med*. 195:789–794.

17. Douek, D.C., R.D. McFarland, P.H. Keiser, E.A. Gage, J.M. Massey, B.F. Haynes, M.A. Polis, A.T. Haase, M.B. Feinberg, J.L. Sullivan, et al. 1998. Changes in thymic function with age and during the treatment of HIV infection. *Nature*. 396:690–695.

18. Pannetier, C., M. Cochet, S. Darche, A. Casrouge, M. Zoller, and P. Kourilsky. 1993. The sizes of the CDR3 hypervariable regions of the murine T-cell receptor beta chains vary as a function of the recombined germ-line segments. *Proc. Natl. Acad. Sci. USA*. 90:4319–4323.

19. Gorski, J., M. Yassai, X. Zhu, B. Kissela, C. Keever, and N. Flomenberg. 1994. Circulating T cell repertoire complexity in normal individuals and bone marrow recipients analyzed by CDR3 spectratyping: correlation with the immune status. *J. Immunol*. 152:5109–5119.

20. Brenchley, J.M., N.J. Karandikar, M.R. Betts, D.R. Ambrozak, B.J. Hill, L.E. Crotty, J.P. Casazza, J. Kuruppu, S.A. Migueles, M. Connors, et al. 2003. Expression of CD57 defines replicative senescence and antigen-induced apoptotic death of CD8+ T cells. *Blood*. 101:2711–2720.

21. Mackall, C.L., T.A. Fleisher, M.R. Brown, M.P. Andrich, C.C. Chen, I.M. Feuerstein, M.E. Horowitz, I.T. Magrath, A.T. Shad, S.M. Steinberg, et al. 1995. Age, thymopoiesis, and CD4+ T-lymphocyte regeneration after intensive chemotherapy. *N. Engl. J. Med*. 332:143–149.

22. Douek, D.C., R.A. Vescio, M.R. Betts, J.M. Brenchley, B.J. Hill, L. Zhang, J.R. Berenson, R.H. Collins, and R.A. Koup. 2000. Assessment of thymic output in adults after haematopoietic stem-cell transplantation and prediction of T-cell reconstitution. *Lancet*. 355:1875–1881.

23. Hug, A., M. Korporal, I. Schroder, J. Haas, K. Glatz, B. Storch-Hagenlocher, and B. Wildemann. 2003. Thymic export function and T cell homeostasis in patients with relapsing remitting multiple sclerosis. *J. Immunol*. 171:432–437.

24. Tanchot, C., A. Le Campion, B. Martin, S. Leaument, N. Dautigny, and B. Lucas. 2002. Conversion of naive T cells to a memory-like phenotype in lymphopenic hosts is not related to a homeostatic mechanism that fills the peripheral naive T cell pool. *J. Immunol*. 168:5042–5046.

25. Ge, Q., H. Hu, H.N. Eisen, and J. Chen. 2002. Different contributions of thymopoiesis and homeostasis-driven proliferation to the reconstitution of naive and memory T cell compartments. *Proc. Natl. Acad. Sci. USA*. 99:2989–2994.

26. Weiner, H.L., and J.A. Cohen. 2002. Treatment of multiple sclerosis with cyclophosphamide: critical review of clinical and immunologic effects. *Mult. Scler*. 8:142–154.

27. Gbadamosi, J., C. Buhmann, W. Tessmer, A. Moench, F. Haag, and C. Heesen. 2003. Effects of mitoxantrone on multiple sclerosis patients' lymphocyte subpopulations and production of immunoglobulin, TNF-alpha and IL-10. *Eur. Neurol*. 49:137–141.

28. Peggs, K.S., S. Verfuerth, A. Pizzey, N. Khan, P. Moss, A.H. Goldstone, K. Yong, and S. Mackinnon. 2003. Reconstitution of T-cell repertoire after autologous stem cell transplantation: influence of CD34 selection and cytomegalovirus infection. *Biol. Blood Marrow Transplant*. 9:198–205.

29. Gorochov, G., P. Debre, V. Leblond, B. Sadat-Sowti, F. Sigaux, and B. Autran. 1994. Oligoclonal expansion of CD8+ CD57+ T cells with restricted T-cell receptor beta chain variability after bone marrow transplantation. *Blood*. 83:587–595.

30. Morley, J.K., F.M. Batliwalla, R. Hingorani, and P.K. Gregersen. 1995. Oligoclonal CD8+ T cells are preferentially expanded in the CD57+ subset. *J. Immunol*. 154:6182–6190.

31. Monteiro, J., F. Batliwalla, H. Ostrer, and P.K. Gregersen. 1996. Shortened telomeres in clonally expanded CD28-CD8+ T cells imply a replicative history that is distinct from their CD28+CD8+ counterparts. *J. Immunol*. 156:3587–3590.

32. Hakim, F.T., R. Cepeda, S. Kaimei, C.L. Mackall, N. McAtee, J. Zujewski, K. Cowan, and R.E. Gress. 1997. Constraints on CD4 recovery postchemotherapy in adults: thymic insufficiency and apoptotic decline of expanded peripheral CD4 cells. *Blood*. 90:3789–3798.

33. Singh, R.K., M.L. Varney, S. Buyukberber, K. Ino, A.G. Ageitos, E. Reed, S. Tarantolo, and J.E. Talmadge. 1999. Fas-FasL-mediated CD4+ T-cell apoptosis following stem cell transplantation. *Cancer Res*. 59:3107–3111.

34. Mackall, C.L., T.A. Fleisher, M.R. Brown, M.P. Andrich, C.C. Chen, I.M. Feuerstein, I.T. Magrath, L.H. Wexler, D.S. Dimitrov, and R.E. Gress. 1997. Distinctions between CD8+ and CD4+ T-cell regenerative pathways result in prolonged T-cell subset imbalance after intensive chemotherapy. *Blood*. 89:3700–3707.

35. Effros, R.B., and G. Pawelec. 1997. Replicative senescence of T cells: does the Hayflick Limit lead to immune exhaustion? *Immunol. Today*. 18:450–454.

36. Selin, L.K., M.Y. Lin, K.A. Kraemer, D.M. Pardoll, J.P. Schneck, S.M. Varga, P.A. Santolucito, A.K. Pinto, and R.M. Welsh. 1999. Attrition of T cell memory: selective loss of LCMV epitope-specific memory CD8 T cells following infections with heterologous viruses. *Immunity*. 11:733–742.

37. Autran, B., V. Leblond, B. Sadat-Sowti, E. Lefranc, P. Got, L. Sutton, J.L. Binet, and P. Debre. 1991. A soluble factor released by CD8+ CD57+ lymphocytes from bone marrow transplanted patients inhibits cell-mediated cytolysis. *Blood*. 77:2237–2241.

38. Sadat-Sowti, B., P. Debre, L. Mollet, L. Quint, F. Hadida, V. Leblond,

G. Bismuth, and B. Autran. 1994. An inhibitor of cytotoxic functions produced by CD8+CD57+ T lymphocytes from patients suffering from AIDS and immunosuppressed bone marrow recipients. *Eur. J. Immunol.* 24:2882–2888.

39. Mollet, L., B. Sadat-Sowti, J. Duntze, V. Leblond, F. Bergeron, V. Calvez, C. Katlama, P. Debre, and B. Autran. 1998. CD8hi+CD57+ T lymphocytes are enriched in antigen-specific T cells capable of down-modulating cytotoxic activity. *Int. Immunol.* 10:311–323.

40. Poser, C.M., D.W. Paty, L.C. Scheinberg, W.I. McDonald, F.A. Davis, G.C. Ebers, K.P. Johnson, K.P. Sibley, D.H. Silberberg, and W.W. Tourtellotte. 1983. New diagnostic criteria for multiple sclerosis: guidelines for research protocols. *Ann. Neurol.* 13:227–231.

41. Kurtzke, J.F. 1983. Rating neurologic impairment in multiple sclerosis: an expanded disability status scale. *Neurology.* 33:1444–1452.

42. Burt, R.K., B.A. Cohen, E. Russell, K. Spero, A. Joshi, Y. Oyama, W.J. Karpus, K. Luo, B. Jovanovic, A. Traynor, et al. 2003. Hematopoietic stem cell transplantation for progressive multiple sclerosis: failure of a total body irradiation-based conditioning regimen to prevent disease progression in patients with high disability scores. *Blood.* 102:2373–2378.

43. Nash, R.A., J.D. Bowen, P.A. McSweeney, S.Z. Pavletic, K.R. Maravilla, M.S. Park, J. Storek, K.M. Sullivan, J. Al-Omaishi, J.R. Corboy, et al. 2003. High-dose immunosuppressive therapy and autologous peripheral blood stem cell transplantation for severe multiple sclerosis. *Blood.* 102:2364–2372.

44. Inglese, M., G.L. Mancardi, E. Pagani, M.A. Rocca, A. Murialdo, R. Saccardi, G. Comi, and M. Filippi. 2004. Brain tissue loss occurs after suppression of enhancement in patients with multiple sclerosis treated with autologous haematopoietic stem cell transplantation. *J. Neurol. Neurosurg. Psychiatry.* 75:643–644.

45. Mancardi, G.L., R. Saccardi, M. Filippi, F. Gualandi, A. Murialdo, M. Inglese, M.G. Marrosu, G. Meucci, L. Massacesi, A. Lugaresi, et al. 2001. Autologous hematopoietic stem cell transplantation suppresses Gd-enhanced MRI activity in MS. *Neurology.* 57:62–68.

46. Carreras, E., A. Saiz, P. Marin, C. Martinez, M. Rovira, N. Villamor, M. Aymerich, M. Lozano, F. Fernandez-Aviles, A. Urbano-Izpizua, et al. 2003. CD34+ selected autologous peripheral blood stem cell transplantation for multiple sclerosis: report of toxicity and treatment results at one year of follow-up in 15 patients. *Haematologica.* 88:306–314.

47. Saccardi, R., G.L. Mancardi, A. Solari, A. Bosi, P. Bruzzi, P. Di Bartolomeo, A. Donelli, M. Filippi, A. Guerrasio, F. Gualandi, et al. 2004. Autologous HSCT for severe progressive Multiple Sclerosis in a multicenter trial: impact on disease activity and quality of life. *Blood.* 10.1182/blood-2004-08-3205.

48. Muraro, P.A., M. Jacobsen, A. Necker, J.W. Nagle, R. Gaber, N. Sommer, R. Martin, and B. Hemmer. 2000. Rapid identification of local T cell expansion in inflammatory organ diseases by flow cytometric T cell receptor Vb analysis. *J. Immunol. Meth.* 246:131–143.

49. Arden, B., S.P. Clark, D. Kabelitz, and T.W. Mak. 1995. Human T-cell receptor variable gene segment families. *Immunogenetics.* 42:455–500.